jove

# Low-cost Polyethylene Terephthalate Lamination Microfluidics Designs for Multiplexed Zebrafish Imaging

**Shelly Tan**[1], **Xiaoguang Zhu**[2], **Jeremiah J. Zartman**[3,4], **Qing Deng**[1]

[1] Department of Biological Sciences, Purdue University [2] Bindley Bioscience Center, Purdue University [3] Department of Chemical and Biomolecular Engineering, University of Notre Dame [4] Department of Biological Sciences, University of Notre Dame

**Corresponding Author**

**Qing Deng**
qingdeng@purdue.edu

**Citation**

Tan, S., Zhu, X., Zartman, J.J., Deng, Q. Low-cost Polyethylene Terephthalate Lamination Microfluidics Designs for Multiplexed Zebrafish Imaging. *J. Vis. Exp.* (211), e67313, doi:10.3791/67313 (2024).

**Date Published**

September 27, 2024

**DOI**

10.3791/67313

**URL**

jove.com/video/67313

## Abstract

Zebrafish embryos are transparent and thus uniquely suited for noninvasive intravital imaging of fundamental processes, such as wound healing and immune cell migration. Microfluidic devices are used for entrapment to support long-term imaging of multicellular organisms, including zebrafish. However, the fabrication of these devices using soft lithography requires specialized facilities and competency in 3D printing, which may not be accessible to every lab. Our adaptation of a previously developed low-cost polyethylene terephthalate lamination method for constructing microfluidic devices increases accessibility by enabling design fabrication and iteration for a fraction of the technical investment of conventional techniques. We use a device made with this method, the Rotational Assistant for Danio Imaging of Subsequent Healing (RADISH), to accommodate drug treatment, manual wounding, and long-term imaging of up to four embryos in the same field of view. With this new design, we successfully capture gross morphological characteristics of the calcium signal around laser ablation and manual transection wounds for multiple embryos in the 2 h immediately following injury, as well as neutrophil recruitment to the wound edge for 24 h.

## Introduction

The ability to respond adequately to injury is critical to the survival of every organism at every scale, from a single cell to multiple tissues. Wounding and its associated responses, such as phagocyte recruitment to damaged areas[1] are, therefore, significant topics in cell and tissue biology. Wounds are sensed immediately after the tissue barrier is breached, causing a tissue gradient response involving wound contraction[2,3] that coordinates wound healing and subsequent regrowth[4]. Due to the mechanical nature of this contraction, tools used during experimentation must not physically impede the movement of cells near the injury site.

Zebrafish embryos are an excellent model for studying development and disease, including the vertebrate wound response, due to their ease of care, genetic tractability, and optical transparency[5,6]. However, immobilizing the whole organism for an extended period is needed to study the

longer-term behavior of cells near an injury site. Embedding embryos in low-melt agarose is sufficient for short-term imaging of unwounded tissue. However, the surrounding gel matrix restricts the contraction and relaxation of wounds and impedes the growth of the developing embryos over time[7,8,9].

Microfluidics devices can immobilize zebrafish embryos at different developmental stages[10,11,12,13,14,15,16], and some, such as the zWEDGI[7], accommodate manual wounding. However, there are several drawbacks to available device designs. For example, many devices printed directly on plastic are incompatible with imaging on inverted microscope systems due to poor optical transparency. Furthermore, parallel channels allow multipositional imaging[10,11], but the physical movement of the microscope stage introduces lag in image acquisition. Repeated iteration and optimization to solve these issues are difficult when considering the financial and technical investment required for every new design, especially for current gold-standard methods of device fabrication using polydimethylsiloxane (PDMS) soft lithography. The very first step, the creation of a master mold, often requires knowledge of 3D modeling software, access to specialized fabrication equipment, and (depending on the material used) an additional antiadhesion treatment such as silanization before the mold is ever used. Curing the PDMS once poured takes at least one hour at high temperatures, and generally, must be done under a vacuum or with a clamp for best results, often in a clean room[7,17,18]. As in developmental biology, these costs can rapidly prove prohibitive for experiments requiring many unique microfluidic environments across multiple models.

Of available alternative construction materials, polyethylene terephthalate (PET) is durable, nontoxic, and easy to manipulate. PET sheets are widely available plastic lamination pouches carried at most office supply stores, with pre-applied thermally-activated adhesive (generally ethylene vinyl acetate). By shaping these PET sheets using commercially available craft cutters (i.e., computer-controlled cutting plotters designed for home crafters) and adhering the layers to one another using standard thermal lamination equipment, a wide range of potential designs can be quickly generated and iterated. We have therefore adapted a previously described method of design and construction involving stacked PET[18] to create the Rotational Assistant for Danio Imaging of Subsequent Healing (RADISH) (**Figure 1A,B**). A rotational arrangement of several approximately wedge-shaped restraining channels optimizes proximity while allowing room for manual tail fin transection, accommodating imaging immediately after wounding and simultaneous long-term imaging of multiple wounded zebrafish embryos within the same field of view. Additionally, this construciton method drastically reduces the upfront capital costs and the time required for device construction while maintaining reusability.

## Protocol

This study used 3 days post fertilization (dpf) embryos but can be designed to use 2-14 dpf embryos. The zebrafish experiment was conducted by internationally accepted standards. The Animal Care and Use Protocol was approved by The Purdue Animal Care and Use Committee (PACUC), adhering to the Guidelines for using Zebrafish in the NIH Intramural Research Program (protocol number: 1401001018).

## 1. Assembly of the PET microfluidics device

NOTE: Any part of this protocol may be paused at any time except for steps 1.8 and 1.9, which are sensitive to the drying time of cyanoacrylate.

1. Design the pattern for the device in the software of choice (e.g., Adobe Illustrator, **Figure 1A**). Depending on the age and size of the embryo, adjust the width of the channel and the size of the central imaging chamber for best fit.
    1. Save each layer as an individual image file with identical dimensions. Name each file so that the thickness of the sheet to be used and the order of assembly are evident.
2. Initialize the cutting machine according to the manufacturer's instructions.
3. Upload each designed pattern to the design software for cutting.
    1. In the design workspace, select the newly uploaded designs. Group patterns intended for the same thickness of PET sheet together in the same cut (**Figure 2A**). If necessary, readjust the size of the patterns in the design software to the correct dimensions.
    2. Confirm the number and type of patterns in the cut, then select the **cut material**.
    NOTE: PET sheets may not be a material choice in the design software, including under names such as "plastic laminating pouch." Any material of similar thickness and texture (e.g., transparency sheets or non-adhesive vinyl) can be selected instead.
    3. Attach the PET sheets to the cutting mat, pressing firmly to remove air bubbles, and load the mat into the cutting machine. Follow onscreen instructions to prompt the cutting machine to begin the cut.
    4. Remove finished cuts from the cutting mat. If necessary, adjust cut patterns using a craft knife or scalpel blade.
    NOTE: The image files used to create the RADISH design (**Figure 1A**) are available for download as vector and PNG file formats (**Supplemental File 1**). If the cutting machine is lifting, tearing, or failing to cut cleanly through the PET sheet, consider replacing the cutting mat.
4. Align the layers on coverslip glass, unassisted or with precut registration marks. If multiple layers can be fastened in place together before lamination, align them simultaneously.
5. Secure the layers with office tape to avoid shifting during lamination (**Figure 2B**). Depending on the device size and laminator capacity, mount small designs to a larger backing with more tape to avoid jamming or clogging the laminator feed (**Figure 2C**).
NOTE: The backing used in lamination is NOT the same as the cutting mat, and serves primarily to provide traction for the laminator. Any heat-resistant material of negligible thickness will work as a backing (including, but not limited to, cardstock, folded office paper, or a larger PET sheet).
6. Turn on the laminator and laminate according to the manufacturer's instructions. Remove office tape before aligning the next layer (**Figure 2D**).
7. Repeat steps 1.4 through 1.6 until all layers have been adhered to.

8. Secure the device to a 35 mm dish drilled with a ¾" hole using cyanoacrylate glue (**Figure 2E,F**). Adjust the shape and type of the dish according to experimental needs (e.g., any container large enough to accommodate the device-one well in a 24-well plate or a larger Petri dish). Use enough glue to seal the device fully to the dish without flooding it.

   NOTE: Securing the device to a holding dish is not required for device function.CAUTION: Cyanoacrylate bonds skin and eyes in seconds and irritates the respiratory system, eyes, and skin. Wear hand and eye protection and work in a well-ventilated area.

9. Waterproof the PET laminate by thoroughly coating the outer device edges with cyanoacrylate glue (**Figure 2F**). Use enough glue to fully cover the outer edges. Allow the glue to cure for at least 2 h before use.

   NOTE: **Ensure adequate room for cyanoacrylate fumes to vent.** The buildup of fumes may cause cyanoacrylate to deposit on the device, obscuring optically transparent material.

## 2. Positioning of the embryos within the RADISH and preparation for imaging

1. Raise zebrafish embryos in the standard embryo-rearing medium E3[19]. If necessary, dechorionate embryos at least 1 h before imaging to allow them to flatten. This experiment used embryos at 3 dpf, but embryos can be up to 14 dpf (**Figure 1E**).

2. Stain or treat the embryos according to experimental needs.

   NOTE: In these experiments, cell membranes of the outer epithelial layer were stained where relevant by incubating with 100 nM MemGlow 560.

3. Anesthetize embryos using 164 mg/L MS-222[20].

   NOTE: The exact concentration and anesthetic used may be adjusted according to the experimenter's preference. Anesthetic concentration can be reduced to allow successful development during long-term images (see step 4.1).

4. Fill the holding dish containing the mounted device with 5 mL of E3 containing 164 mg/L MS-222.

5. Using a transfer pipette, deposit one anesthetized embryo into each holding chamber of the device. Ensure that the embryos remain submerged in liquid for the duration of imaging.

   NOTE: The RADISH design can immobilize 1-4 embryos.

6. Using a hair loop, orient the embryos such that the tail of the embryo protrudes into the central imaging chamber and the yolk is securely immobilized in the wedge-shaped channel (**Figure 1C**).

   NOTE: Orienting embryos may be performed under a stereomicroscope for ease of manipulation.

7. If desired, secure the head of the embryo by adding 1.5% low-melt agarose into the holding chamber using a micropipette.

8. Move the device with embryos to the imaging system of choice to commence imaging.

## 3. Imaging of calcium transients after wounding

NOTE: This section and Section 4 are optional and provided as potential sample experiments.

1. Select the appropriate system and objective for imaging.

   NOTE: Here, an inverted laser scanning confocal was equipped with a 20x objective.

2. Adjust the sample focus and imaging parameters (e.g., **laser power: 5**, **gain: 90**, **pinhole size : 2 AU**, exposure time [**scan speed: 1 frame/s**]) for optimal signal-to-noise ratio and acquisition speed.
   NOTE: It is recommended that samples be prefocused and parameters for each channel on the imaging system of choice be adjusted **before wounding** to reduce the lag between wound formation and image acquisition.
3. Wound a *Tg(krt4:Gal4, UAS:GCaMP6f) x (cdh1-dTomato)*$^{xt18}$[21,22] embryo.
   1. To wound the embryo via manual transection, apply pressure with a scalpel blade across the tail fin tissue at the tip of the notochord under a stereomicroscope (**Video 1**), then return the device to the stage.
      CAUTION: Applying excessive pressure with the scalpel blade can crack the underlying glass. If the glass cracks, discard the device and restart from Step 1.2.
   2. To wound the embryo via laser stimulation, define a region of interest (ROI) near the edge of the tail fin fold and stimulate according to the available laser power.
      NOTE: Here, **a laser power** of **2.4 W** for **30 s** at **800 nm** was sufficient to induce a full-thickness wound.
4. Image at room temperature using **GFP** (excitation 488 nm, emission 510 nm) and **RFP** (excitation 561 nm, emission 610 nm) channels using a **frame interval** of **1 min** for a total of 1 h.
5. (Optional): If necessary, release the embryos for retrieval after imaging via gentle suction near the head using a transfer pipette or swirling the dish.

### 4. Imaging of neutrophil recruitment after wounding

1. At least 1 h before imaging, transfer the embryos to E3 containing half the standard concentration of anesthetic, in this case, 82 mg/L MS-222.
2. Select the appropriate objective for imaging (here, an inverted laser scanning confocal equipped with a 10x objective).
3. Adjust the sample focus and imaging parameters (e.g., **laser power: 5**, **gain: 90, pinhole size: 2 AU, exposure time** [**scan speed: 0.5 frame/s**])) for optimal signal-to-noise ratio and acquisition speed.
   NOTE: It is recommended that samples be prefocused and parameters for each channel on the imaging system of choice be adjusted **before wounding** to reduce the lag between wound formation and image acquisition.
4. Wound four *Tol2(mpx:Dendra2)*[23] embryos via manual transection by applying pressure with a scalpel blade across the tail fin tissue under a stereomicroscope, then return the device to the stage.
5. Capture the image on the **GFP** (excitation 488 nm, emission 510 nm) channel at room temperature using a **5 min frame interval** for **24 h**.
6. If necessary, release the embryos for retrieval after imaging via gentle suction near the head using a transfer pipette or swirling the dish.

## Representative Results

For comparison of image quality produced by a laser scanning confocal with and without the aid of the RADISH, embryos expressing the intensiometric calcium biosensor GCaMP6f[22,24] in the outer epithelial layer were stained

using MemGlow 560 and imaged with an inverted laser scanning confocal covering the entire thickness of the tail fin fold at a time interval of 1 min per frame (**Video 2**). Without the device (**Figure 3A**), samples drifted significantly and displayed banding artifacts, resulting from limiting the Z-stack to 25 slices to fit within the specified temporal resolution compared to imaging with the device (**Figure 3B**). The RADISH was further used to examine calcium transients immediately after wounding in embryos expressing *Tg(krt4:Gal4, UAS:GCaMP6f) x (cdh1-dTomato)*$^{xt18}$[21], highlighting endogenous E-cadherin in red and cytoplasmic calcium in the apical epithelium in green. Embryos were wounded parallel to the sides of the central chamber using a scalpel blade (**Figure 4A** and **Video 3**) or by direct laser ablation with an IR laser (**Figure 4B**), then imaged through the full thickness of the tail fin fold.

To demonstrate the effectiveness of the RADISH for longer-term imaging, we investigated immune cell recruitment to the wound edge for 24 h after wounding. Four zebrafish embryos at 3 dpf expressing *Tol2(mpx:Dendra2)* to label neutrophils in green[23] were wounded by tail transection and imaged for 24 consecutive hours (**Figure 5**). Imaging artifacts typically associated with late 3 dpf to 4 dpf embryos, such as tilting and floating, were notably absent (**Video 4**), and tissue regrowth continued unimpeded for the experiment. Neutrophil recruitment to the wound edge continues throughout the image (**Figure 5B**), with most migrating cells leaving by 24 h post wounding (**Figure 5C**), consistent with expected inflammation resolution[25,26].

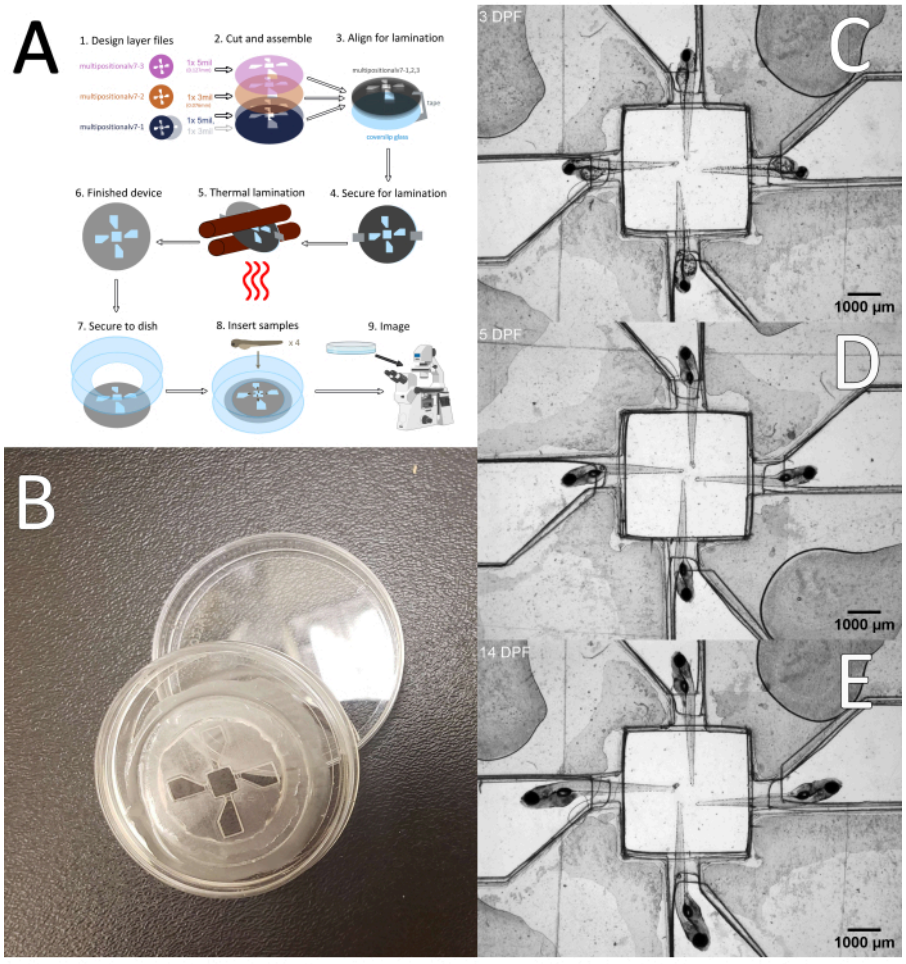


**Figure 1: Design and use of PET laminate microfluidics device (RADISH).** (**A**) Schematic illustrating individual PET layers' arrangement and thickness, assembly, and device mounting and use. (**B**) Final product, mounted in a ¾" cutout in a 35 mm dish. (**C**) 3 dpf embryos, (**D**) 5 dpf embryos, (**E**) 14 dpf embryos housed inside the device. Scale bars = 1,000 µm (**C**,**D**,**E**). Abbreviations: PET = polyethylene terephthalate; RADISH = Rotational Assistant for Danio Imaging of Subsequent Healing; dpf = days post fertilization. Please click here to view a larger version of this figure.

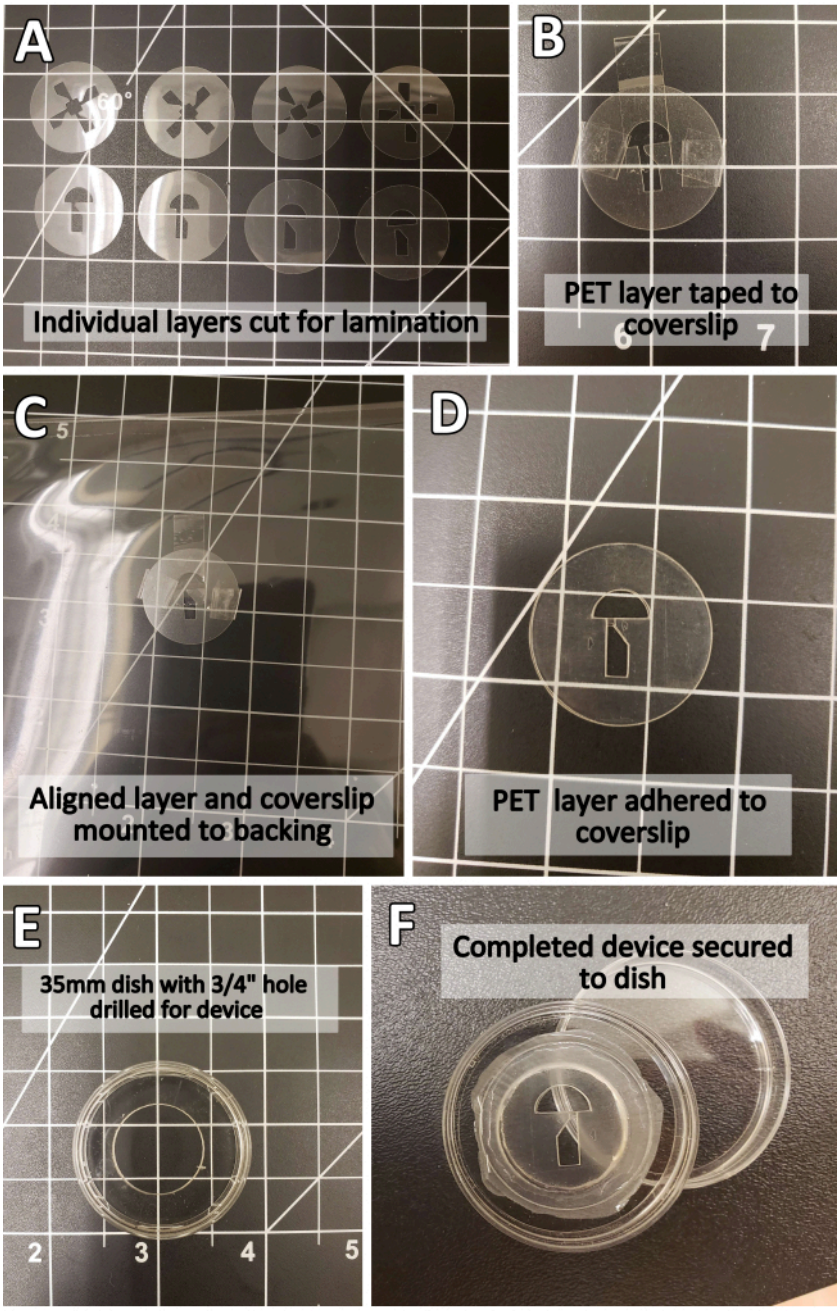


**Figure 2: Step-by-step photographic illustration of PET device assembly.** (**A**) Individual PET layers before lamination. (**B**) PET layer secured to 25 mm coverslip using office tape. (**C**) Device-in-progress secured to a plastic backing for lamination. (**D**) Completed PET laminate device. (**E**) Modified 35 mm dish before device mounting. (**F**) Completed device. Abbreviation: PET = polyethylene terephthalate. Please click here to view a larger version of this figure.

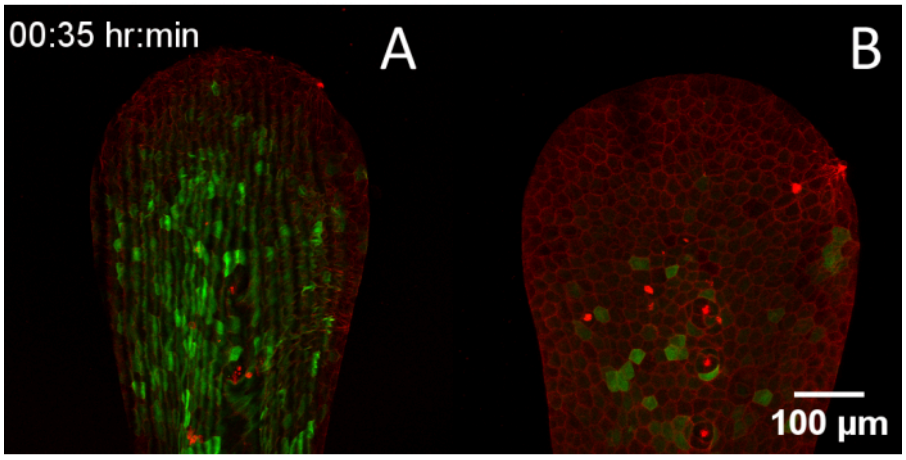


**Figure 3: Improved quality of laser scanning confocal images of 3 dpf embryos in the RADISH design.** (**A**) Representative image of 3 dpf *Tg(krt4:Gal4, UAS:GCaMP6f)* embryo stained with MemGlow 560 without using the RADISH. (**B**) Representative image of *Tg(krt4:Gal4, UAS:GCaMP6f)* embryo stained with MemGlow 560 mounted in the RADISH. Scale bar = 100 µm. Abbreviations: RADISH = Rotational Assistant for Danio Imaging of Subsequent Healing; dpf = days post fertilization. Please click here to view a larger version of this figure.

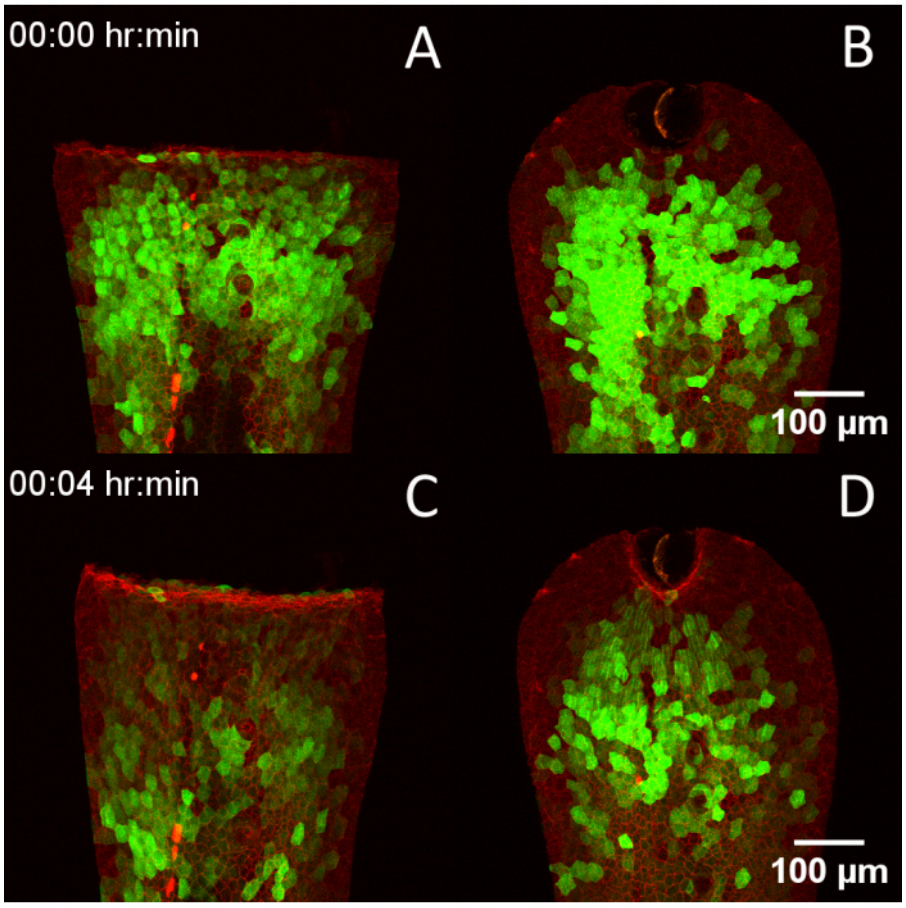


**Figure 4: Compatibility of the RADISH design with multiple wounding techniques.** (**A**) 3 dpf *Tg(krt4:Gal4, UAS:GCaMP6f) x (cdh1-dTomato)*$^{xt18}$ embryo wounded via manual tailfin transection. (**B**) Embryo wounded via laser ablation. (**C**,**D**) The same embryos 4 min later, showing the progression of calcium transients after wounding. Scale bars = 100 µm. Abbreviations: RADISH = Rotational Assistant for Danio Imaging of Subsequent Healing; dpf = days post fertilization. Please click here to view a larger version of this figure.

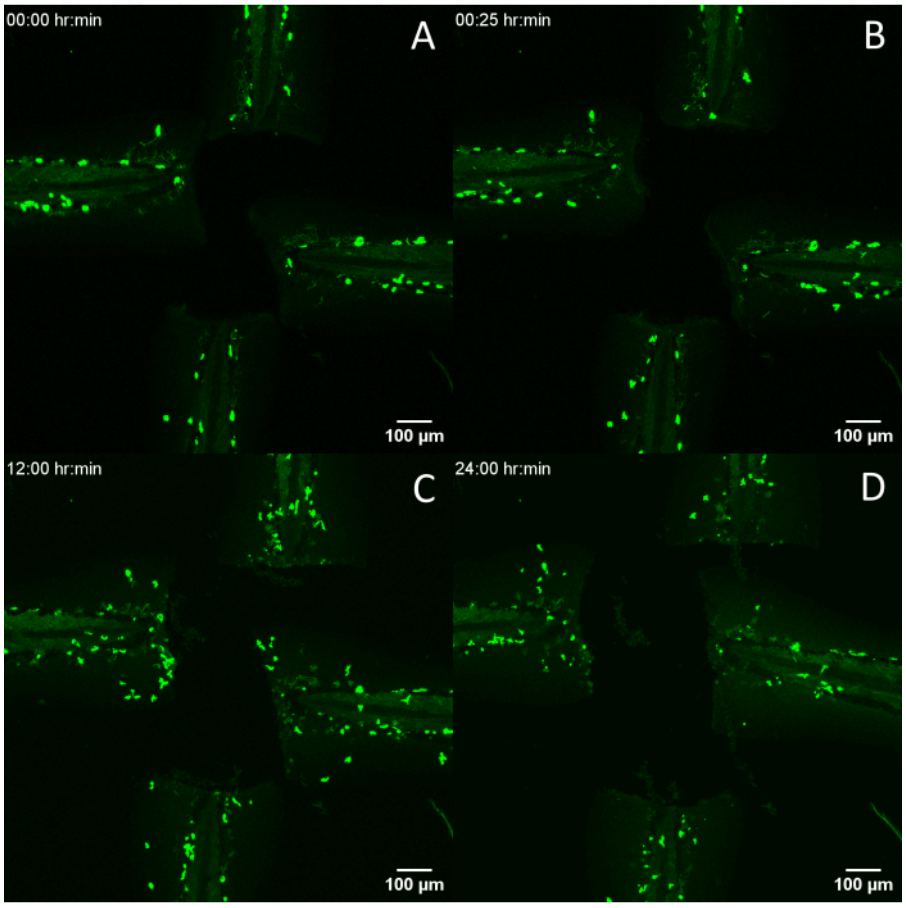


**Figure 5: Long-term entrapment of embryos for imaging of phagocyte migration.** (**A**) *Tol2(mpx:Dendra2)* embryos immediately post wounding, and the same embryos (**B**) 25 min, (**C**) 12 h, and (**D**) 24 h later. Scale bars = 100 µm. Please click here to view a larger version of this figure.

**Supplemental File 1: Vector and PNG files for RADISH device design as shown in Figure 1A.** Please click here to download this File.

**Video 1: Brightfield video of manual tailfin transection using RADISH device design.** Abbreviation: RADISH = Rotational Assistant for Danio Imaging of Subsequent Healing. Please click here to download this Video.

**Video 2: Comparison of unmounted versus mounted 3 dpf *Tg(krt4:Gal4, UAS:GCaMP6f)* embryos from Figure 3, acquired at 1 frame/min.** Please click here to download this Video.

**Video 3: Calcium transients in *Tg(krt4:Gal4, UAS:GCaMP6f) x (cdh1-dTomato)$^{xt18}$* embryos wounded via scalpel transection or laser ablation from Figure 4, acquired at 1 frame/min.** Please click here to download this Video.

**Video 4: Long-term imaging of leukocyte recruitment and tail fin regeneration in *Tol2(mpx:Dendra2)***

**embryos**. Abbreviations: RADISH = Rotational Assistant for Danio Imaging of Subsequent Healing; hpw = hours post wounding. Please click here to download this Video.

## Discussion

The core premise of the PET lamination method involves cost reduction and minimization of technical barriers to entry compared to traditional means of creating microfluidic devices, such as soft lithography or PDMS molding. As such, the only critical steps in this protocol are the accurate alignment of PET layers during lamination and waterproofing of the device edges after construction. All other parts of the method may be modified according to experimental needs (e.g., if immobilization of younger or older embryos is required, the thickness of the PET layers can be adjusted to narrow or widen the channel accordingly). Designs can be created in any shape and laminated onto any base material as long as the material is heat-safe and thin enough to be sent through the laminator[18,27]. As PET sheets are cut using commercially available craft cutters, which read two-dimensional rather than three-dimensional image files, the design and iteration of any given device require only the ability to manipulate black and white shapes in an image editing program, dramatically decreasing the difficulty. This flexibility in software choice and the commercial availability of materials used represent a dramatic increase in the accessibility of microfluidics devices in general, enabling their use in any lab or classroom for an upfront cost of less than $500 at the time of writing this paper, compared to over $2000 in starting equipment costs for PDMS mold fabrication[17].

Furthermore, the time required to create a single useable device using this method is dramatically reduced compared to typical soft lithography. Assuming familiarity with the requisite software, one unique PET laminate microfluidic device can be conceptualized, manufactured, and immediately used in ~3 h, *including* the curing time of cyanoacrylate. Iteration takes even less, depending on the scale of edits needed to the original design files, and multiple variant devices can be made in parallel with minimal additional time invested and no extra equipment. Although devices created using this method are less durable than those made with PDMS for a variety of reasons (including adhesive failure and internal stresses for shapes with many layers and long aspect ratios), their inexpensive nature and scalable fabrication mean that they are far more easily replaced. As commercial craft cutters are marketed with the ability to repeat the same precise cut over and over and PET has no expiration date, the individual layers of a completed design can be pre-prepared in bulk for assembly and use at any point in the future, further reducing the overall time investment required.

However, speed and variability come at the cost of precision. The main limitation of PET lamination compared with traditional PDMS molding is spatial resolution. Commercial craft cutters often struggle with sharp angles on shapes smaller than approximately 500 µm, and PET lamination sheets are not available at thicknesses under 33 µm (not including the thickness of the adhesive itself, which is not included in the measurement on the package), significantly limiting the scale at which this technique can be applied. The maximum number of layers is also restricted by the size of the laminator, which may vary from manufacturer to manufacturer.

The final version of the protocol, including variations in registration and alignment technique, materials suppliers, and software, will largely depend on user preference. However, the method's accessibility and overall flexibility reduce the cost of adaptation. Individual users are

encouraged to iterate as much as necessary to adapt the approach to their unique needs.

## Disclosures

The authors have no conflicts of interest to disclose.

## Acknowledgments

The work was supported by research funding from the National Institutes of Health (R35GM119787 to QD). This work is based upon efforts supported by EMBRIO Institute, NSF contract #2120200, a National Science Foundation (NSF) Biology Integration Institute. Confocal imaging was performed at the Purdue Imaging Facility. We thank Dr. Guangjun Zhang (Purdue University) for providing the Tg(UAS:GCaMP6f) line. We thank Dr. David Tobin (Duke University) for providing the (cdh1-tdtomato)xt18 line.

## References

1. De Oliveira, S., Rosowski, E. E., Huttenlocher, A. Neutrophil migration in infection and wound repair: going forward in reverse. *Nat Rev Immunol.* **16** (6), 378-391 (2016).
2. Xu, S., Hsiao, T. I., Chisholm, A. D. The wounded worm. *Worm.* **1** (2), 134-138 (2012).
3. Belacortu, Y., Paricio, N. Drosophila as a model of wound healing and tissue regeneration in vertebrates. *Dev Dyn.* **240** (11), 2379-2404 (2011).
4. Yoo, S. K., Freisinger, C. M., LeBert, D. C., Huttenlocher, A. Early redox, Src family kinase, and calcium signaling integrate wound responses and tissue regeneration in zebrafish. *J Cell Biol.* **199** (2), 225-234 (2012).
5. Kawakami, A., Fukazawa, T., Takeda, H. Early fin primordia of zebrafish larvae regenerate by a similar growth control mechanism with adult regeneration. *Dev Dyn.* **231** (4), 693-699 (2004).
6. Gault, W. J., Enyedi, B., Niethammer, P. Osmotic surveillance mediates rapid wound closure through nucleotide release. *J Cell Biol.* **207** (6), 767-782 (2014).
7. Huemer, K. et al. zWEDGI: Wounding and entrapment device for imaging live zebrafish larvae. *Zebrafish.* **14** (1), 42-50 (2017).
8. Kaufmann, A., Mickoleit, M., Weber, M., Huisken, J. Multilayer mounting enables long-term imaging of zebrafish development in a light sheet microscope. *Development.* **139** (17), 3242-3247 (2012).
9. Hirsinger, E., Steventon, B. A versatile mounting method for long term imaging of zebrafish development. *J Vis Exp.* (119), e55210 (2017).
10. Wielhouwer, E. M. et al. Zebrafish embryo development in a microfluidic flow-through system. *Lab Chip.* **11** (10), 1815-1824 (2011).
11. Khalili, A., Rezai, P. Microfluidic devices for embryonic and larval zebrafish studies. *Brief Funct Genomics.* **18** (6), 419-432 (2019).
12. Choudhury, D. et al. Fish and Chips: a microfluidic perfusion platform for monitoring zebrafish development. *Lab Chip.* **12** (5), 892-900 (2012).
13. Zhang, G. et al. An integrated microfluidic system for zebrafish larva organs injection. *Proceedings IECON 2017 - 43rd Annual Conference of the IEEE Industrial Electronics Society.* 2017-January, 8563-8566 (2017).
14. Erickstad, M., Hale, L. A., Chalasani, S. H., Groisman, A. A microfluidic system for studying the behavior of zebrafish larvae under acute hypoxia. *Lab Chip.* **15** (3), 857-866 (2015).

15. Mani, K., Hsieh, Y. C., Panigrahi, B., Chen, C. Y. A noninvasive light driven technique integrated microfluidics for zebrafish larvae transportation. *Biomicrofluidics.* **12** (2), 021101 (2018).

16. Lee, Y., Seo, H. W., Lee, K. J., Jang, J. W., Kim, S. A microfluidic system for stable and continuous EEG monitoring from multiple larval zebrafish. *Sensors (Basel).* **20** (20), 5903 (2020).

17. Sonnen, K. F., Merten, C. A. Microfluidics as an emerging precision tool in developmental biology. *Dev Cell.* **48** (3), 293-311 (2019).

18. Levis, M. et al. Microfluidics on the fly: Inexpensive rapid fabrication of thermally laminated microfluidic devices for live imaging and multimodal perturbations of multicellular systems. *Biomicrofluidics.* **13** (2), 024111 (2019).

19. E3 medium (for zebrafish embryos). *Cold Spring Harbor Protocols.* **2011** (10), pdb.rec66449 (2011).

20. Matthews, M., Varga, Z. M. Anesthesia and euthanasia in zebrafish. *ILAR J.* **53** (2), 192-204 (2012).

21. Cronan, M. R., Tobin, D. M. Endogenous tagging at the cdh1 locus for live visualization of E-cadherin dynamics. *Zebrafish.* **16** (3), 324 (2019).

22. Thiele, T. R., Donovan, J. C., Baier, H. Descending control of swim posture by a midbrain nucleus in zebrafish. *Neuron.* **83** (3), 679-691 (2014).

23. Yoo, S. K., Huttenlocher, A. Spatiotemporal photolabeling of neutrophil trafficking during inflammation in live zebrafish. *J Leukoc Biol.* **89** (5), 661-667 (2011).

24. Chen, T. W. et al. Ultrasensitive fluorescent proteins for imaging neuronal activity. *Nature.* **499** (7458), 295-300 (2013).

25. Li, L., Yan, B., Shi, Y.-Q., Zhang, W.-Q., Wen, Z.-L. Live imaging reveals differing roles of macrophages and neutrophils during zebrafish tail fin regeneration. *J Biol Chem.* **287** (30), 25353-25360 (2012).

26. Mathias, J. R. et al. Resolution of inflammation by retrograde chemotaxis of neutrophils in transgenic zebrafish. *J Leukoc Biol.* **80**, 1281-1288 (2006).

27. Levis, M., Ontiveros, F., Juan, J., Kavanagh, A., Zartman, J. J. Rapid fabrication of custom microfluidic devices for research and educational applications. *J Vis Exp.* **2019** (2019).